IOP PUBLISHING NANOTECHNOLOGY
Nanotechnology **20** (2009) 455101 (9pp) doi:10.1088/0957-4484/20/45/455101

Differential plasma protein binding to metal oxide nanoparticles

Zhou J Deng[1], Gysell Mortimer[1], Tara Schiller[2], Anthony Musumeci[2], Darren Martin[2] and Rodney F Minchin[1,3]

[1] School of Biomedical Sciences, University of Queensland, Brisbane, QLD 4072, Australia
[2] Australian Institute for Bioengineering and Nanotechnology, University of Queensland, Brisbane, QLD 4072, Australia

E-mail: r.minchin@uq.edu.au

Received 3 June 2009
Published 13 October 2009
Online at stacks.iop.org/Nano/20/455101

Abstract

Nanoparticles rapidly interact with the proteins present in biological fluids, such as blood. The proteins that are adsorbed onto the surface potentially dictate the biokinetics of the nanomaterials and their fate *in vivo*. Using nanoparticles with different sizes and surface characteristics, studies have reported the effects of physicochemical properties on the composition of adsorbed plasma proteins. However, to date, few studies have been conducted focusing on the nanoparticles that are commonly exposed to the general public, such as the metal oxides. Using previously established ultracentrifugation approaches, two-dimensional gel electrophoresis and mass spectrometry, the current study investigated the binding of human plasma proteins to commercially available titanium dioxide, silicon dioxide and zinc oxide nanoparticles. We found that, despite these particles having similar surface charges in buffer, they bound different plasma proteins. For TiO_2, the shape of the nanoparticles was also an important determinant of protein binding. Agglomeration in water was observed for all of the nanoparticles and both TiO_2 and ZnO further agglomerated in biological media. This led to an increase in the amount and number of different proteins bound to these nanoparticles. Proteins with important biological functions were identified, including immunoglobulins, lipoproteins, acute-phase proteins and proteins involved in complement pathways and coagulation. These results provide important insights into which human plasma proteins bind to particular metal oxide nanoparticles. Because protein absorption to nanoparticles may determine their interaction with cells and tissues *in vivo*, understanding how and why plasma proteins are adsorbed to these particles may be important for understanding their biological responses.

1. Introduction

Plasma proteins play an important role in recognizing foreign bodies that enter the circulation. Specific proteins are involved in eliciting an immunological response to pathogens or in assisting their clearance by the reticuloendothelial system, particularly in the liver [46, 42, 17]. Recently, the binding of plasma proteins to nanoparticles has been identified as a critical step in determining their fate *in vivo* [29, 37]. The interactive surface that is recognized by cells and other biological structures is often determined by the protein corona that forms rapidly in plasma, surrounding the nanoparticle [5]. The nature of the proteins that interact with specific nanoparticles depends on the particle size as well as their surface characteristics [28]. Surface curvature, for example, can significantly affect the secondary structure of proteins absorbed onto nanoparticles [27]. For some proteins, this can lead to a loss of function [20] or the unfolding of epitopes not normally exposed to the surrounding biological medium [31]. The binding of albumin to single-walled carbon nanotubes appears to promote their uptake by the scavenger receptor in RAW 264.7 cells [12], which is consistent with the high localization of these particles in the liver following intravenous administration [8]. Similarly, the binding of apolipoproteins to poly(butylcyanoacrylate) nanoparticles may assist in their transcytosis across the blood–brain barrier [21].

[3] Author to whom any correspondence should be addressed.

Detailed analysis using precisely engineered nanoparticles has shown that nanoparticles develop a 'soft' and 'hard' protein corona depending on the affinity of the protein for the nanomaterial [28]. Low affinity proteins exchange rapidly between the surface of the nanoparticle and the surrounding solution while high affinity proteins remain bound for longer. This can lead to time-dependent changes in the protein corona as more abundant, low affinity proteins are replaced by less abundant, high affinity proteins [30]. Hydrophobicity is an important determinant of the amount of protein that binds to latex nanoparticles [3, 14]. Predictably, surface modification with hydrophilic molecules such as polyethylene glycol can dramatically decrease protein binding [41]. However, other forces such as electrostatic interaction may determine the nature and extent of binding, depending on the surface characteristics of the nanoparticles [30]. Proteins with isoelectric points (pI) less than 5.5 predominantly bind to nanoparticles with a basic surface while proteins with pI greater than 5.5 bind to particles with an acidic surface [13]. Because of the complexities of protein–nanoparticle interactions, it may be necessary and appropriate to analyse individual particles on a case-by-case basis to understand how proteins determine their fate in the circulation [45, 35].

Nanosized metal-oxide-related products are used in many commercial applications such as photocatalysis, solar cells, cosmetic products including sunscreens, automotive parts, surface coatings and medical products. Therefore, these nanomaterials have already been extensively exposed to the public to varying extents. Toxicological studies suggest some metal oxide nanomaterials could have detrimental biological effects [36, 16, 6, 23]. Once entered into the circulation, these nanoparticles should adsorb plasma proteins that may dictate their biological fate. A better understanding of the nature of this protein absorption is necessary. Therefore, in the present study, we have compared the binding of human plasma proteins to three of the most commonly used and widely available metal oxide nanoparticles: titanium dioxide (TiO_2), silicon dioxide (SiO_2) and zinc oxide (ZnO).

2. Experimental details

2.1. Metal oxide nanoparticles

Commercial TiO_2 nanoparticles (Degussa P25) were purchased from Evonik Degussa, SiO_2 nanoparticles (S5130) were purchased from Sigma-Aldrich and ZnO nanoparticles (Nanosun™ 99/30) were kindly supplied by Microniser, Australia. ZnO particles coated with polymethylsilsesquioxane (ZinClear_40CCT) were obtained from Advanced Powder Technologies, Australia.

2.2. Synthesis of TiO_2 nanorods and nanotubes

TiO_2 nanotubes were synthesized using a method adapted from [33]. Briefly, the hydrothermal treatment of Degussa P25 (10 mg ml^{-1}) in a high temperature hydrothermal pressure vessel was undertaken at 150 °C for 20 h. The nanotubes were washed with 0.1 M HCl until ~pH 7 was reached and then with MilliQ H_2O. TiO_2 nanorods were synthesized through a similar procedure to that outlined by Rabatic *et al* [38]. In short, the hydrothermal treatment of TiO_2 nanorods ([TiO_2] = 0.081–0.0081 M) in a high temperature hydrothermal pressure vessel at 250 °C for 2 h.

2.3. Nanoparticle characterization

Metal oxide nanoparticles were dispersed in MilliQ water. To facilitate the dispersion of the nanoparticles, bath sonication was applied for 30 min. The hydrodynamic sizes and zeta potentials of the nanoparticle in water and buffer (150 mM NaCl, 10 mM phosphate, pH 7.4) were analysed by DLS using a Zetasizer Nano ZS (Malvern Instruments, Malvern, UK). Transmission electron microscopy (TEM) images were taken using a JEOL 1010 fitted with a SIS megaview slow-scan camera to assess nanoparticle size, shape and purity. Images were acquired at an accelerating voltage of 80 keV on either 200 mesh holey carbon grids or formvar carbon-coated copper grids. All particle size estimations were made from several TEM images with an average of at least 100 different nanoparticles (+standard deviation).

2.4. Human plasma samples

Human plasma samples were obtained from eight healthy individuals according to institutional bioethics approval. Blood from each donor was collected in sodium citrate and centrifuged for 5 min at 800g to pellet the blood cells. The supernatants (plasma) were combined and stored in aliquots at −80 °C. On thawing, the plasma was centrifuged for 2 min at 18 000g before use.

2.5. Incubation of nanoparticle with plasma

Nanoparticles in water were transferred into buffer (150 mM sodium chloride and 10 mM phosphate, pH 7) and incubated with 1% plasma at 37 °C for 5 min to 4 h. After incubation, unbound proteins were separated from the nanoparticles by centrifuging at 50 000g for 40 min at 4 °C. Plasma without nanoparticles was used as a control to ensure there was no protein precipitation. Particle pellets were carefully washed with the buffer four times, and resuspended in SDS sample buffer to final concentrations of 2 mg ml^{-1} of nanoparticles, with 2% SDS, 5% β-mercaptoethanol, 10% glycerol and 62.5 mM Tris-HCl. Samples were then heated at 95 °C for 5 min to desorb particle-bound proteins [3, 25, 28]. The prepared samples were separated by gel electrophoreses. All experiments were conducted at least in triplicate. Due to the agglomeration in aqueous medium, the calculation of total surface area for the nanoparticles was not practical. Thus, nanoparticle masses were used to normalize the final loading volumes.

2.6. One-dimensional (1D) and two-dimensional (2D) gel electrophoresis

All prepared samples contained nanoparticles at a final concentration of 2 mg ml^{-1}. For 1D gel electrophoresis, 20 μl

of sample (equivalent to 40 μg nanoparticles) was separated on a 12% SDS–polyacrylamide (SDS–PAGE) gel. The gels were run at a constant voltage of 200 V for 35 min, and stained with Sypro Ruby protein stains (Bio-Rad). For 2D gel electrophoresis, 40 μl of the prepared samples (equivalent to 80 μg nanoparticles) was mixed with 7 M urea, 2 M thiourea, 4% CHAPS, 0.4% DTT and 1% Bio-Lyte 3/10 ampholyte (Bio-Rad) in a final volume of 300 μl. The sample was then applied to a 17 cm pH 3–10 Readystrip™ IPG strip (Bio-Rad) and actively rehydrated at 50 V overnight using a Protean® IEF cell. Isoelectric focusing was performed for a total of 45 kVh at 20 °C. The IPG strips were reduced with 1% DDT in equilibration buffer (100 mM Tris-HCl, 6 M urea, 30% glycerol, 2% SDS) for 15 min and then alkylated with 4% iodoacetamide in equilibration buffer for a further 15 min. Equilibrated IPG strips were transferred onto 17 cm 8–15% SDS–polyacrylamide gradient gels and sealed with 1% agarose. The gels were run using a Protean® II xi cell apparatus at 15 W/gel until the dye front migrated to the bottom of the gel. 2D gels were silver-stained according to published methods [18]. All gels were imaged with a ChemiDoc XRS system using Quantity One 4.5.0 software (Bio-Rad). Proteins were identified by their isoelectric points and mass using the ExPASy database (http://au.expasy.org/swiss-2dpage/viewer).

2.7. Protein identification by mass spectrometry

Protein bands from 1D SDS–PAGE gels were excised and in-gel digested with trypsin according to established procedures [24]. The peptide extracts were analysed by LC-MS/MS on an Agilent 1100 Nano HPLC (San Jose, CA, USA) coupled to a QStar Elite mass spectrometer (Applied Biosystems) equipped with a nanoelectrospray ion source. The spectra were acquired and processed using Analyst QS 2.0 software (Applied Biosystems). The database searching for protein identification was carried out using Protein Pilot 2.0.1 (Applied Biosystem).

3. Results and discussion

3.1. Characterization of metal oxide nanoparticles

The commercial TiO_2, SiO_2 and ZnO nanoparticles have average primary particle sizes of 21 nm, 7 nm and 30 nm, respectively, as reported by the manufacturers. These sizes were verified by TEM (figure 1(A)). All nanoparticles became agglomerated in buffer with an average hydrodynamic diameter ranging from 300 to 450 nm determined by DLS. Sonication for as long as 2 h did not change the extent of agglomeration (data not shown). When the metal oxide nanoparticles were diluted in buffer, increased agglomeration was observed (figure 1(B)). This may be due to the increase in ionic strength resulting in decreased electrical-double-layer repulsive energy between the nanoparticles [47]. Buffer-dispersed nanoparticles were prepared at two different concentrations: 10 and 500 $\mu g\,ml^{-1}$. For TiO_2 and ZnO, increased concentrations resulted in increased agglomeration, which was not seen for SiO_2 (figure 1(B)). In buffer, the average zeta potentials for TiO_2, SiO_2 and ZnO were -26 ± 6 mV, -26 ± 6 mV and -24 ± 2 mV, respectively (figure 1(C)). This was unaffected by nanoparticle concentration.

Table 1. Identification of proteins bound to nanoparticles by 1D gel electrophoresis and mass spectrometry.

Band[a]	Nanoparticle	Proteins
1	TiO_2	Albumin, fibrinogen (alpha chain), kininogen-1, histidine-rich glycoprotein, complement C9
2	TiO_2	Kininogen-1
3	TiO_2	Fibrinogen (beta chain), Ig heavy chain (gamma), fetuin A, vitronectin
4	TiO_2	Apolipoprotein A1, complement C1q
5	SiO_2	Albumin, fibrinogen (alpha chain), complement C8, Ig heavy chain (kappa)
6	SiO_2	Fibrinogen (alpha, beta, gamma chains)
7	SiO_2	Fibrinogen (beta, gamma chain), Ig heavy chain (gamma)
8	SiO_2	Apolipoprotein A
9	ZnO	Alpha-2-macroglobulin, pregnancy zone protein
10	ZnO	Ig heavy chain (mu), transferrin
11	ZnO	Albumin, Ig heavy chain (gamma)
12	ZnO	Ig heavy chain (alpha), Ig heavy chain (mu)
13	ZnO	Alpha-1 antichymotrypsin, Ig heavy chain (gamma)
14	ZnO	Apolipoprotein A1, immunoglobulin J chain

[a] The bands refer to the numbers shown in figure 2(B).

3.2. Plasma protein binding by metal oxide nanoparticles

The binding of proteins to each nanoparticle is shown in figure 2. There were no detectable proteins in plasma samples centrifuged in the absence of nanoparticles (data not shown). General binding reached equilibrium within the first 5 min of incubation, as the protein patterns did not change for up to 4 h (figure 2(A)). Overall, the results support previous observations that nanoparticles can bind many different plasma proteins to varying extents [5]. Protein binding to TiO_2 and SiO_2 was very similar but notably different to that observed for ZnO despite comparable surface charges. The type and extent of protein bound to TiO_2 and ZnO varied with nanoparticle concentrations (figure 2(B)). Since the zeta potentials for these nanoparticles did not change (figure 1(C)), the difference in protein binding is most likely due to the greater agglomeration sizes at the higher nanoparticle concentrations. This is supported by the observed protein binding characteristics of SiO_2, which did not agglomerate and showed very little difference in protein binding at the different concentrations (figure 2(B), centre panel).

Siliconate-treated ZnO nanoparticles were also obtained from a commercial source. These nanoparticles showed no detectable binding of plasma proteins compared to normal ZnO nanoparticles (figure 2(C)) indicating that surface modification of the nanoparticles can markedly influence protein binding. Moreover, it also shows that the proteins detected in figures 2(A) and (B) did not simply co-sediment with the nanoparticles.

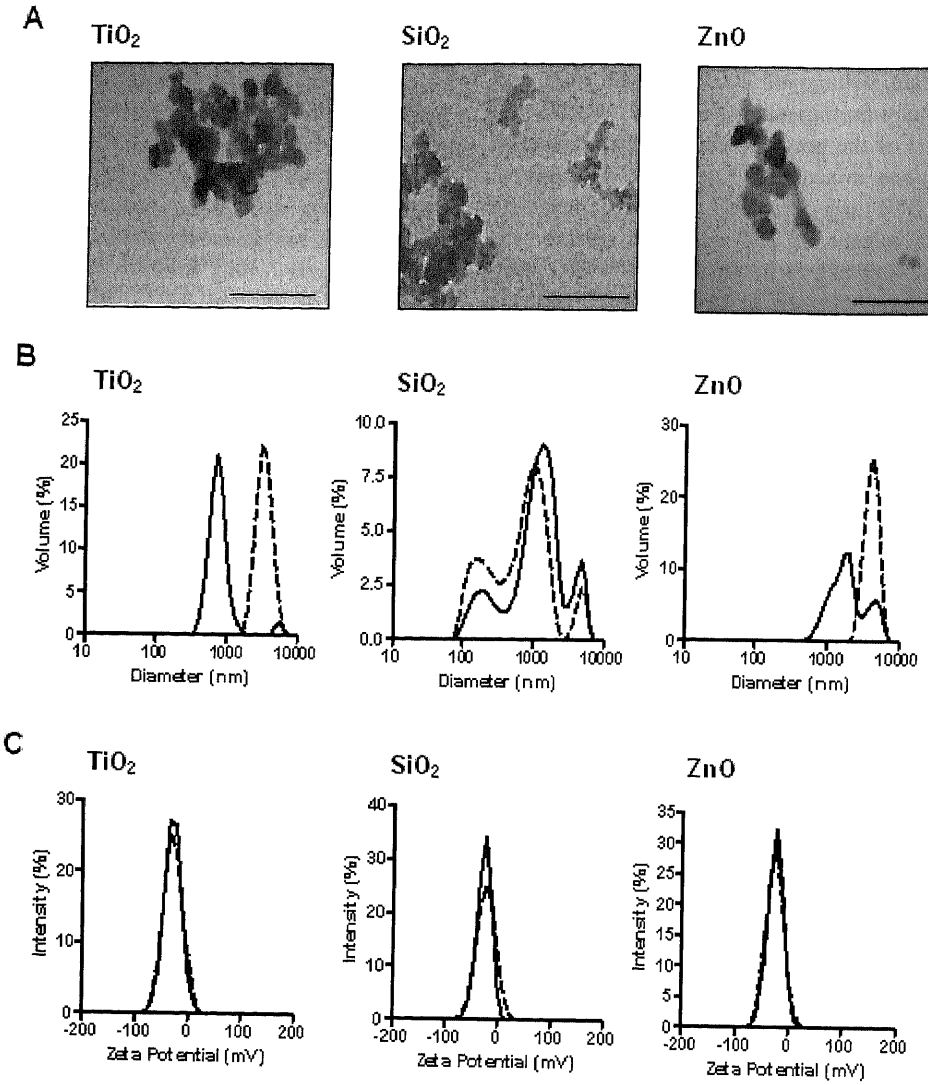

Figure 1. Characterization of commercial metal oxide nanoparticles. (A) TEM images of TiO_2 (Degussa P25), SiO_2 (S5130) and ZnO (Nanosun™ 99/30) nanoparticles. Bar = 100 nm. (B) Hydrodynamic particle diameters of the different nanoparticles in buffer determined by dynamic light scattering. Solid lines = 10 μg ml^{-1} and dashed lines = 500 μg ml^{-1}. (C) Zeta potential of the different nanoparticles in buffer: solid lines = 10 μg ml^{-1} and dashed lines = 500 μg ml^{-1}.

To identify major proteins bound to the different metal oxides, slices were excised from gels prepared at a nanoparticle concentration of 10 μg ml^{-1} and analysed by mass spectrometry. The different slices are shown in figure 2(B) and the associated proteins are listed in table 1. Apolipoprotein A1 bound to all three metal oxides, as did albumin, immunoglobulins and fibrinogen. Transferrin (band 10), alpha-2 macroglobulin and pregnancy zone protein (band 9) were detected only with ZnO. The immunoglobulin IgM also bound to ZnO nanoparticles, possibly in the pentameric form since the immunoglobulin J chain was also present (band 14). Various components of the complement system were identified bound to TiO_2 (bands 1 and 4). Taken together, these results show that the metal oxides interact with numerous plasma proteins. Moreover, these proteins can vary upon changes in agglomeration state. Although qualitatively different, the complexity of the protein corona around the metal oxide nanoparticles agrees with that reported for polymeric nanoparticles of different sizes and surface characteristics [28]. The nanoparticle–protein corona potentially dictates the fate of the nanoparticles once in the systemic circulation. Therefore, the degree of nanoparticle agglomeration may, to some extent, dictate the resultant biodistribution by affecting cell surface protein binding.

3.3. Identification of proteins by 2D gel electrophoresis

Because the migration of most plasma proteins on 2D gels has been well characterized and their specific characteristics are available in various databases (http://au.expasy.org/swiss-2dpage/viewer), we analysed protein binding to each metal oxide by 2D gel electrophoresis using a nanoparticle concentration of 10 μg ml^{-1} (figure 3). Individual proteins or protein classes were identified by their respective molecular weights and pI and a list of proteins bound to each metal oxide is shown in table 2. Most of the proteins identified by mass

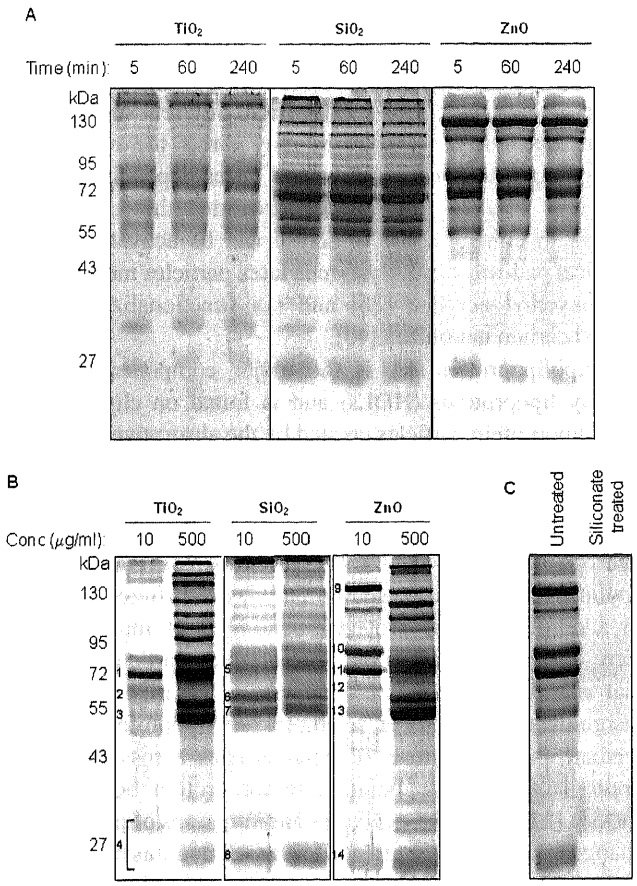

Figure 2. Gel electrophoresis of nanoparticle-bound human plasma proteins. (A) Effect of time of incubation on protein binding. (B) Effect of concentration of protein binding. The numbers on the gels represent regions of each gel that were excised and analysed by mass spectrometry. (C) Effect of silicone treatment on the binding of plasma proteins to ZnO nanoparticles.

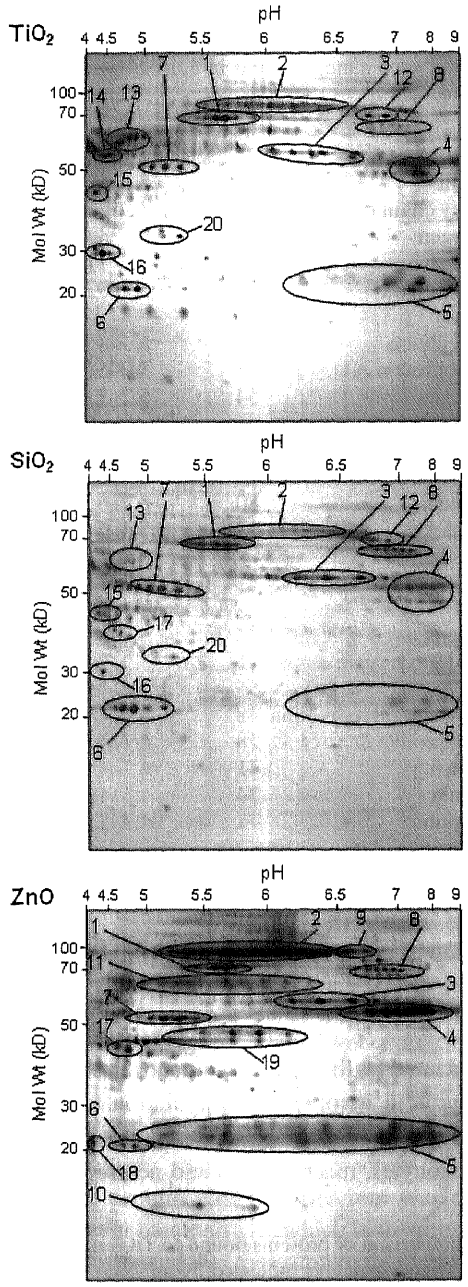

Figure 3. 2D gel electrophoresis of proteins bound to metal oxide nanoparticles. Proteins were identified from the plasma protein database of Expasy and are described in table 2.

spectroscopy (table 1) were also identified on the 2D gels. With the exception of an unknown protein (ID 17), proteins bound to TiO_2 were also bound to SiO_2 (figure 3, upper and middle panels). Albumin, the most abundant protein in plasma, was associated with each metal oxide, but at a relatively low level. The immunoglobulins IgM (table 2, ID 2) and IgG (table 2, ID 4) bound to all three particles. IgG and IgM to a lesser extent, can act as an opsonin and promote phagocytosis of nanoparticles by macrophages or other phagocytic cells such as hepatic Kupffer cells [34]. This is consistent with published observations that TiO_2 nanoparticles primarily accumulate in the liver following intravenous administration [7]. In addition, both IgG and IgM can activate the complement system, leading to an inflammatory response. In contrast, IgA bound only to ZnO. IgA is secreted into the intestine lumen along with the Ig J chain, which was also bound to ZnO nanoparticles (table 2, ID 18). In the plasma, IgA can interact with the Fcα receptor and promote the release of pro-inflammatory cytokines [11]. In a recent comprehensive review, Dobrovolskaia and McNeil outlined the susceptibility of the immune system to various engineered nanoparticles [10]. They summarized current knowledge on how size and charge can determine the interaction of nanomaterials with blood components. They also observed that, in general, positively charged particles are more likely to elicit an immune reaction compared to negatively charged particles *in vitro*. However, *in vivo* this may not be the case for the nanoparticles that bind immunoglobulins to a high degree. Negatively charged ZnO nanoparticles can elicit a pronounced inflammatory response in an endothelial cell model in the presence of serum [15]. While some evidence that metal oxide nanoparticles can induce immune responses has been published [1], their effects *in vivo* need further study.

All three nanoparticles appeared to bind fibrinogen (table 2, IDs 3, 7 and 8), a plasma protein commonly

Table 2. Identification of proteins bound to metal oxide nanoparticles by 2D gel electrophoresis. Presence of the protein in the 2D gels for each nanoparticle is indicated by an 'X'.

ID[a]	Protein	Mol. wt.[b] (kD)	pI[b]	TiO_2	SiO_2	ZnO
1	Albumin	67	5.6–5.9	X	X	X
2	Ig heavy chain (mu)	81	5.9–6.1	X	X	X
3	Fibrinogen (beta chain)	55	6.1–6.6	X	X	X
4	Ig heavy chain (gamma)	51	6.2–8.5	X	X	X
5	Ig light chains	25	5.7–8.5	X	X	X
6	Apolipoprotein A1	23	5.0–5.5	X	X	X
7	Fibrinogen (gamma chain)	54	5.2–5.6	X	X	X
8	Fibrinogen (alpha chain)	66	6.7–7.0	X	X	X
9	Transferrin	80	6.2–6.5			X
10	Haptoglobin (alpha chain)	17	5.4–6.0			X
11	Ig heavy chain (alpha)	63	5.0–5.6			X
12	Complement C3	71	6.5–6.8	X	X	X
13	Alpha-1 antitrypsin	55	4.9–5.1	X	X	
14	Fetuin A	55	4.6–4.7	X		
15	Alpha-2 acid-glycoprotein	48	4.5–4.7	X	X	
16	Apolipoprotein D	28	4.7–4.9	X	X	
17	Unknown	41	4.7–4.9		X	X
18	Ig J chain	24	4.5–4.6			X
19	Haptoglobin (beta chain)	44	4.7–5.4			X
20	Clusterin	37	4.7–5.2	X	X	

[a] ID refers to numbers shown in figure 3.

[b] Mol. wt. and pI values from http://au.expasy.org/swiss-2dpage/viewer.

found associated with various nanoparticles [5]. Fibrinogen is a glycoprotein involved in coagulation. It also binds to foreign surfaces and promotes attachment of immune cells such as monocytes, macrophages and neutrophils. Fibrinogen binds to CD11/CD18 on phagocytes, delays apoptosis and enhances antibody-dependent cellular cytotoxicity and phagocytosis [44, 39]. Complement C3 (table 2, ID 12) also promotes neutrophil attachment to different surfaces [32]. Taken together, these proteins may direct the metal oxide nanoparticles to specific blood cell types depending on their degree of binding. It has been reported that complement present in either plasma or serum can be activated through classical pathways by polystyrene latex particles modified with hydroxyethyl acrylate [26] and non-functionalized double-walled carbon nanotubes [40].

Apolipoprotein A1 is the major component of high-density lipoproteins (HDLs) and is found on chylomicrons, large lipoprotein particles created by the absorptive cells of the small intestine [2]. The protein was found to be associated with all three metal oxides. Apolipoproteins have been reported as one of the major plasma proteins adsorbed by particles with hydrophobic surfaces [22, 4]. The flexible hinge region of apolipoprotein A1 can bind to particles of different sizes [9]. In addition to these proteins, a number of minor proteins were observed bound to the different nanoparticles. Proteins that adsorbed at low levels are not necessarily biologically insignificant [28]. For example, apolipoprotein E could mediate the transcytosis of nanoparticles across the blood–brain barrier despite being a minor protein bound to the surface [21]. Both the structures and functions of proteins may change upon adsorption to nanoparticles, and this may result in biological responses that are unexpected [31, 19, 43, 30].

3.4. *Effect of shape on plasma protein binding to TiO_2*

TiO_2 nanorods and nanotubes were synthesized and examined by TEM (figure 4(A)). The nanorods were ellipsoid in shape with average lengths of 75 ± 23 nm and widths of 27 ± 7 nm (i.e. aspect ratio $= 2.8 \pm 0.7$). The nanotubes had an average tube diameter of 9 ± 1 nm. 2D gel electrophoresis showed that these differently shaped materials had different protein binding

Table 3. Comparison of proteins bound to TiO_2 nanoparticles of different shapes by 2D gel electrophoresis. Presence of the protein in the 2D gels for each nanoparticle is indicated by an 'X'.

ID[a]	Protein	Mol. wt.[b] (kD)	pI[b]	Nanospheres[c]	Nanorods	Nanotubes
1	Albumin	67	5.6–5.9	X	X	X
2	Ig heavy chain (mu)	81	5.9–6.1	X	X	X
3	Fibrinogen (beta chain)	55	6.1–6.6	X		X
4	Ig heavy chain (gamma)	51	6.2–8.5	X	X	
5	Ig light chains	25	5.7–8.5	X	X	X
6	Apolipoprotein A1	23	5.0–5.5	X	X	X
7	Fibrinogen (gamma chain)	54	5.2–5.6	X	X	X
8	Fibrinogen (alpha chain)	66	6.7–7.0	X		X
12	Complement C3	71	6.5–6.8	X	X	X
13	Alpha-1 antitrypsin	55	4.9–5.1	X		
14	Fetuin A	55	4.6–4.7	X		
15	Alpha-2 acid-glycoprotein	48	4.5–4.7	X		
16	Apolipoprotein D	28	4.7–4.9	X		
20	Clusterin	37	4.7–5.2	X		

[a] ID refers to numbers shown in figures 3 and 4.

[b] Mol. wt. and pI from http://au.expasy.org/swiss-2dpage/viewer.

[c] Degussa P25 (table 1, figure 2).

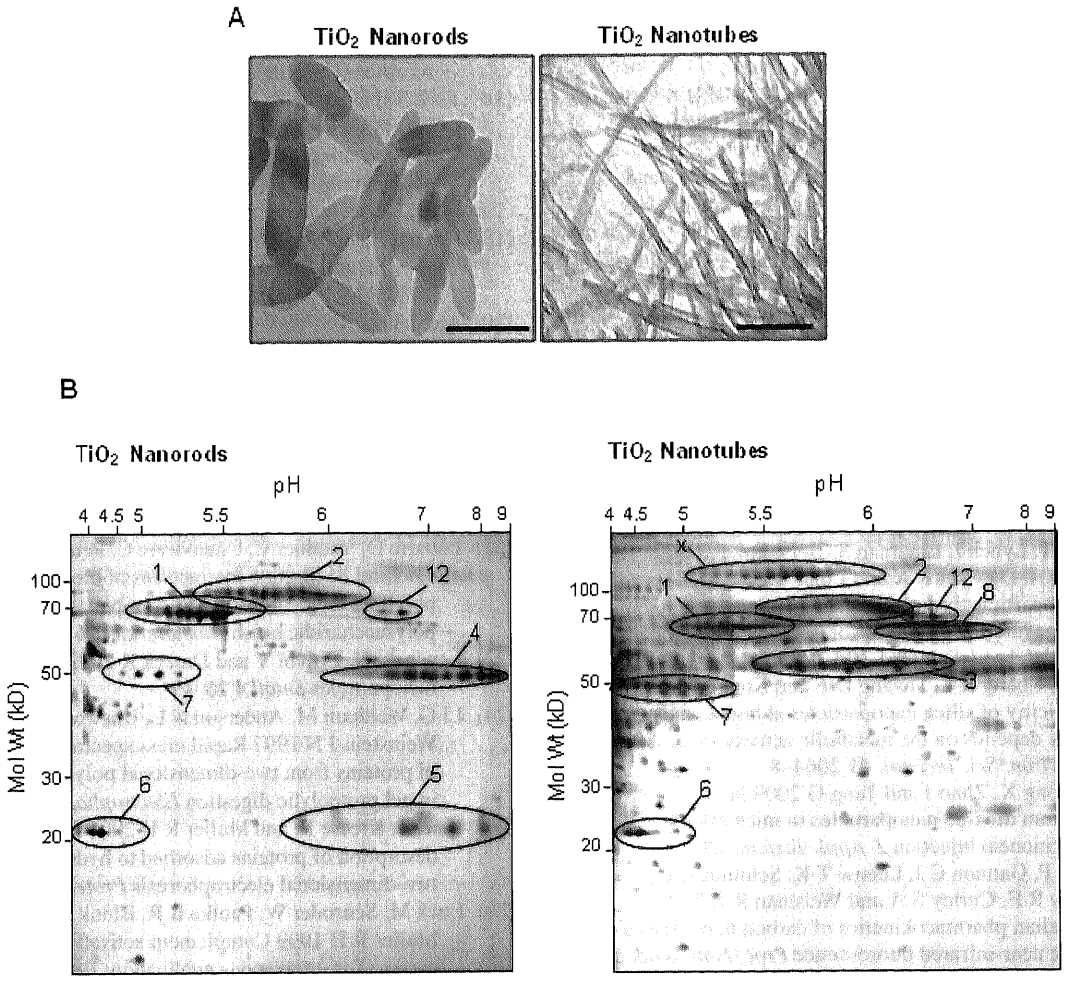

Figure 4. Plasma protein binding to TiO_2 nanorods and nanotubes. (A) TEM images of TiO_2 particles showing rod shape (left panel) and tube shape (right panel). Bar = 100 nm. (B) 2D gel electrophoresis of plasma proteins bound to the different TiO_2 particles. For protein ID, refer to figure 3.

pattern (figure 4(B)). For the nanorods, both IgM and IgG were evident as major bound proteins. By contrast, fibrinogen was the major protein bound to the nanotubes. Albumin and apolipoprotein A1 were seen with both nanoparticles.

Finally, a high molecular weight protein (figure 4(B) ID x), possibly ceruloplasmin, bound to the nanotubes but not to the nanorods. Proteins bound to TiO_2 nanoparticles of different shapes were compared and are summarized in table 3. Clearly, nanospheres (TiO_2, Degussa P25—figure 3) bound qualitatively more proteins compared to the other elongated shapes (figure 4). However, the potential biological implication of this observation is to be elucidated.

4. Conclusions

The current work is the first study to identify and compare the proteins that bind to metal oxide nanoparticles that are commonly found in many commercial products. These included TiO_2, SiO_2 and ZnO and synthetic TiO_2 nanorods and nanotubes. The current work provides much needed information for understanding the initial biological interaction of these metal oxide nanoparticles when entering the circulation of the body, that is, the interaction with proteins in the blood. The protein binding behaviour was distinct for each type of different nanoparticle, which is in agreement with others who have suggested that the complexity of nanoparticle–protein interactions requires each to be examined on a case-by-case basis [45, 35]. Surprisingly, it was found that the adsorption of proteins onto the metal oxide nanoparticles reached equilibrium within the first few minutes of incubation. Moreover, when dispersed in buffer, the surface charge was not the sole determinant of binding because it was similar between the different metal oxides. This work has also shown that the agglomeration state largely affected the protein binding pattern. Because protein binding to nanoparticles can be critical in determining the extent of interaction with cells and tissues *in vivo*, understanding how and why plasma proteins are adsorbed to these particle may be important for understanding their biological responses.

Acknowledgment

This work was supported by a grant from the National Health and Medical Research Council of Australia (grant no. 569594).

References

[1] Arvidsson S, Askendal A and Tengvall P 2007 Blood plasma contact activation on silicon, titanium and aluminium *Biomaterials* **28** 1346–54

[2] Berggard T, Arrigoni G, Olsson O, Fex M, Linse S and James P 2006 140 mouse brain proteins identified by $Ca2^{+}$-calmodulin affinity chromatography and tandem mass spectrometry *J. Proteome Res.* **5** 669–87

[3] Blunk T, Hochstrasser D F, Sanchez J C, Muller B W and Muller R H 1993 Colloidal carriers for intravenous drug targeting: plasma protein adsorption patterns on surface-modified latex particles evaluated by two-dimensional polyacrylamide gel electrophoresis *Electrophoresis* **14** 1382–7

[4] Cedervall T, Lynch I, Foy M, Berggard T, Donnelly S C, Cagney G, Linse S and Dawson K A 2007 Detailed identification of plasma proteins adsorbed on copolymer nanoparticles *Angew. Chem. Int. Edn Engl.* **46** 5754–6

[5] Cedervall T, Lynch I, Lindman S, Berggard T, Thulin E, Nilsson H, Dawson K A and Linse S 2007 Understanding the nanoparticle–protein corona using methods to quantify exchange rates and affinities of proteins for nanoparticles *Proc. Natl Acad. Sci. USA* **104** 2050–5

[6] Chang J S, Chang K L, Hwang D F and Kong Z L 2007 *In vitro* cytotoxicitiy of silica nanoparticles at high concentrations strongly depends on the metabolic activity type of the cell line *Environ. Sci. Technol.* **41** 2064–8

[7] Chen J, Dong X, Zhao J and Tang G 2009 *In vivo* acute toxicity of titanium dioxide nanoparticles to mice after intraperitioneal injection *J. Appl. Toxicol.* **29** 330–7

[8] Cherukuri P, Gannon C J, Leeuw T K, Schmidt H K, Smalley R E, Curley S A and Weisman R B 2006 Mammalian pharmacokinetics of carbon nanotubes using intrinsic near-infrared fluorescence *Proc. Natl Acad. Sci. USA* **103** 18882–6

[9] Cushley R J and Okon M 2002 NMR studies of lipoprotein structure *Annu. Rev. Biophys. Biomol. Struct.* **31** 177–206

[10] Dobrovolskaia M A and McNeil S E 2007 Immunological properties of engineered nanomaterials *Nat. Nanotechnol.* **2** 469–78

[11] Duque N, Gomez-Guerrero C and Egido J 1997 Interaction of IgA with Fc alpha receptors of human mesangial cells activates transcription factor nuclear factor-kappa B and induces expression and synthesis of monocyte chemoattractant protein-1, IL-8, and IFN-inducible protein 10 *J. Immunol.* **159** 3474–82

[12] Dutta D, Sundaram S K, Teeguarden J G, Riley B J, Fifield L S, Jacobs J M, Addleman S R, Kaysen G A, Moudgil B M and Weber T J 2007 Adsorbed proteins influence the biological activity and molecular targeting of nanomaterials *Toxicol. Sci.* **100** 303–15

[13] Gessner A, Lieske A, Paulke B R and Muller R H 2003 Functional groups on polystyrene model nanoparticles: influence on protein adsorption *J. Biomed. Mater. Res.* A **65** 319–26

[14] Gessner A, Waicz R, Lieske A, Paulke B, Mader K and Muller R H 2000 Nanoparticles with decreasing surface hydrophobicities: influence on plasma protein adsorption *Int. J. Pharm.* **196** 245–9

[15] Gojova A, Guo B, Kota R S, Rutledge J C, Kennedy I M and Barakat A I 2007 Induction of inflammation in vascular endothelial cells by metal oxide nanoparticles: effect of particle composition *Environ. Health Perspect.* **115** 403–9

[16] Gurr J R, Wang A S, Chen C H and Jan K Y 2005 Ultrafine titanium dioxide particles in the absence of photoactivation can induce oxidative damage to human bronchial epithelial cells *Toxicology* **213** 66–73

[17] Ishida T, Harashima H and Kiwada H 2001 Interactions of liposomes with cells *in vitro* and *in vivo*: opsonins and receptors *Curr. Drug Metab.* **2** 397–409

[18] Jin L T, Hwang S Y, Yoo G S and Choi J K 2006 A mass spectrometry compatible silver staining method for protein incorporating a new silver sensitizer in sodium dodecyl sulfate–polyacrylamide electrophoresis gels *Proteomics* **6** 2334–7

[19] Kane R S and Stroock A D 2007 Nanobiotechnology: protein–nanomaterial interactions *Biotechnol. Prog.* **23** 316–9

[20] Karajanagi S S, Vertegel A A, Kane R S and Dordick J S 2004 Structure and function of enzymes adsorbed onto single-walled carbon nanotubes *Langmuir* **20** 11594–9

[21] Kreuter J, Shamenkov D, Petrov V, Ramge P, Cychutek K, Koch-Brandt C and Alyautdin R 2002 Apolipoprotein-mediated transport of nanoparticle-bound drugs across the blood-brain barrier *J. Drug Target.* **10** 317–25

[22] Labarre D, Vauthier C, Chauvierre C, Petri B, Muller R and Chehimi M M 2005 Interactions of blood proteins with poly(isobutylcyanoacrylate) nanoparticles decorated with a polysaccharidic brush *Biomaterials* **26** 5075–84

[23] Lewinski N, Colvin V and Drezek R 2008 Cytotoxicity of nanoparticles *Small* **4** 26–49

[24] Li G, Waltham M, Anderson N L, Unsworth E, Treston A and Weinstein J N 1997 Rapid mass spectrometric identification of proteins from two-dimensional polyacrylamide gels after in gel proteolytic digestion *Electrophoresis* **18** 391–402

[25] Lind K, Kresse M and Muller R H 2001 Evaluation of desorption of proteins adsorbed to hydrophilic surfaces by two-dimensional electrophoresis *Proteomics* **1** 1059–66

[26] Luck M, Schroder W, Paulke B R, Blunk T and Muller R H 1999 Complement activation by model drug carriers for intravenous application: determination by two-dimensional electrophoresis *Biomaterials* **20** 2063–8

[27] Lundqvist M, Sethson I and Jonsson B H 2004 Protein adsorption onto silica nanoparticles: conformational changes depend on the particles' curvature and the protein stability *Langmuir* **20** 10639–47

[28] Lundqvist M, Stigler J, Elia G, Lynch I, Cedervall T and Dawson K A 2008 Nanoparticle size and surface properties determine the protein corona with possible implications for biological impacts *Proc. Natl Acad. Sci. USA* **105** 14265–70

[29] Lynch I, Cedervall T, Lundqvist M, Cabaleiro-Lago C, Linse S and Dawson K A 2007 The nanoparticle–protein complex as a biological entity; a complex fluids and surface science challenge for the 21st century *Adv. Colloid Interface Sci.* **134/135** 167–74

[30] Lynch I and Dawson K A 2008 Protein–nanoparticle interactions *Nano Today* **3** 40–7

[31] Lynch I, Dawson K A and Linse S 2006 Detecting cryptic epitopes created by nanoparticles *Sci. STKE* **2006** pe14

[32] McNally A K and Anderson J M 1994 Complement C3 participation in monocyte adhesion to different surfaces *Proc. Natl Acad. Sci. USA* **91** 10119–23

[33] Morgan D L, Zhu H Y, Frost R L and Waclawik E R 2008 Determination of a morphological phase diagram of titania/titanate nanostructures from alkaline hydrothermal treatment of Degussa P25 *Chem. Mater.* **20** 3800–2

[34] Nagayama S, Ogawara K, Fukuoka Y, Higaki K and Kimura T 2007 Time-dependent changes in opsonin amount associated on nanoparticles alter their hepatic uptake characteristics *Int. J. Pharm.* **342** 215–21

[35] Oberdorster G *et al* 2005 Principles for characterizing the potential human health effects from exposure to

nanomaterials: elements of a screening strategy *Part. Fibre Toxicol.* **2** 8

[36] Oberdorster G, Oberdorster E and Oberdorster J 2005 Nanotoxicology: an emerging discipline evolving from studies of ultrafine particles *Environ. Health Perspect.* **113** 823–39

[37] Owens D E 3rd and Peppas N A 2006 Opsonization, biodistribution, and pharmacokinetics of polymeric nanoparticles *Int. J. Pharm.* **307** 93–102

[38] Rabatic B M, Dimitrijevic N M, Cook R E, Saponjic Z V and Rajh T 2006 Spatially confined corner defects induce chemical functionality of TiO_2 nanorods *Adv. Mater.* **18** 1033

[39] Rubel C, Fernandez G C, Dran G, Bompadre M B, Isturiz M A and Palermo M S 2001 Fibrinogen promotes neutrophil activation and delays apoptosis *J. Immunol.* **166** 2002–10

[40] Salvador-Morales C, Flahaut E, Sim E, Sloan J, Green M L and Sim R B 2006 Complement activation and protein adsorption by carbon nanotubes *Mol. Immunol.* **43** 193–201

[41] Sant S, Poulin S and Hildgen P 2008 Effect of polymer architecture on surface properties, plasma protein adsorption, and cellular interactions of pegylated nanoparticles *J. Biomed. Mater. Res.* A **87** 885–95

[42] Scherphof G L and Kamps J A 2001 The role of hepatocytes in the clearance of liposomes from the blood circulation *Prog. Lipid Res.* **40** 149–66

[43] Shen X C, Liou X Y, Ye L P, Liang H and Wang Z Y 2007 Spectroscopic studies on the interaction between human hemoglobin and CdS quantum dots *J. Colloid Interface Sci.* **311** 400–6

[44] Sitrin R G, Pan P M, Srikanth S and Todd R F 3rd 1998 Fibrinogen activates NF-kappa B transcription factors in mononuclear phagocytes *J. Immunol.* **161** 1462–70

[45] Warheit D B, Sayes C M, Reed K L and Swain K A 2008 Health effects related to nanoparticle exposures: environmental, health and safety considerations for assessing hazards and risks *Pharmacol. Ther.* **120** 35–42

[46] Winkelstein J A and Moxon E R 1992 The role of complement in the host's defense against *Haemophilus influenzae* *J. Infect. Dis.* **165** (Suppl 1) S62–5

[47] Zhang Y, Chen Y, Westerhoff P, Hristovski K and Crittenden J C 2008 Stability of commercial metal oxide nanoparticles in water *Water Res.* **42** 2204–12